FRANCE TITANE
The French Titanium Association

CONTINUUM

Prix de Thèse

ÉTUDE MULTI-ÉCHELLE DES ÉVOLUTIONS MICROSTRUCTURALES DANS LES ALLIAGES DE TITANE BIPHASÉS DÉFORMÉS À CHAUD

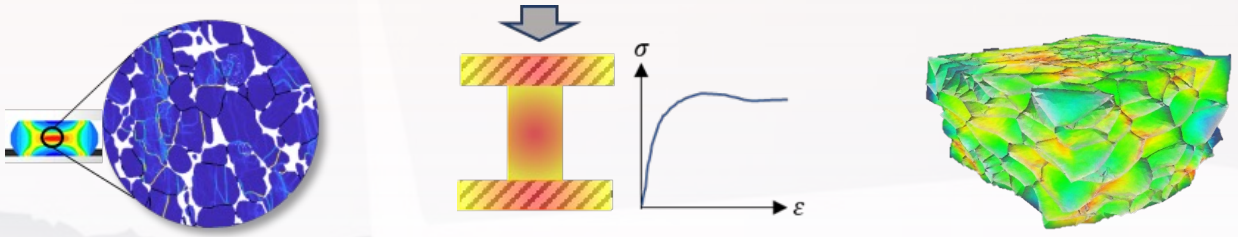

Matheus BROZOVIC GARIGLIO

Encadrants

Nathalie BOZZOLO | *CEMEF*

Daniel PINO MUÑOZ | *CEMEF*

Partenaires industriels

B. DOD | *Airbus*

C. DUMONT | *Aubert & Duval*

J. DELFOSSE et M. PIELLARD | *SafranTech*

Y. MILLET | *Timet*

Cemef · cnrs · MINES ParisTech | PSL · Chimie Paris · INSTITUT P' · AIRBUS · AUBERT&DUVAL · SAFRAN · TIMET

How to obtain the desired properties for aircraft application of Ti alloys?

Ti-6Al-4V
$(\alpha + \beta)$

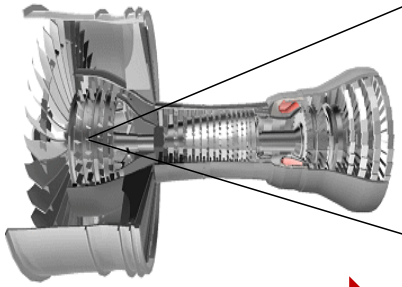

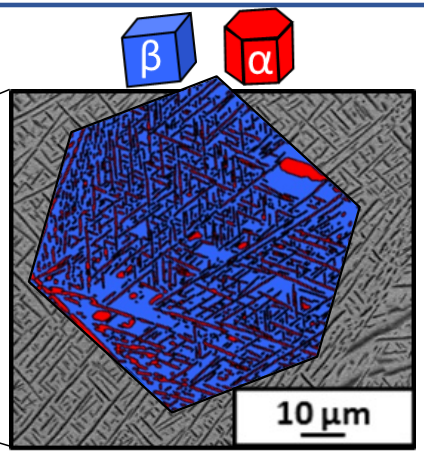

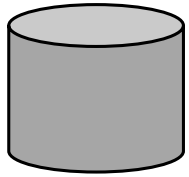

max 315°C → T

Properties | **Microstructures** | **Industrial process (Forging)**

Ti-10V-2Fe-3Al
(metastable-β)

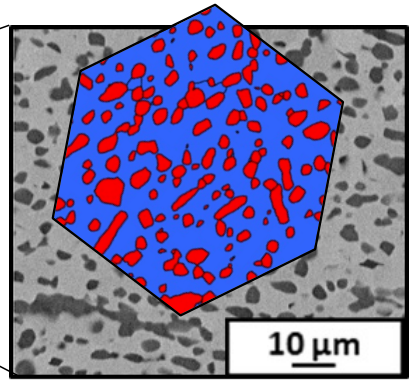

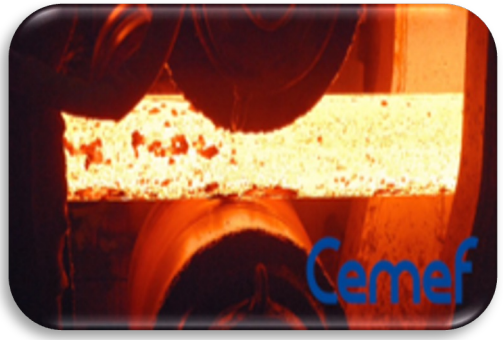

What are the microstructural evolutions during industrial process?

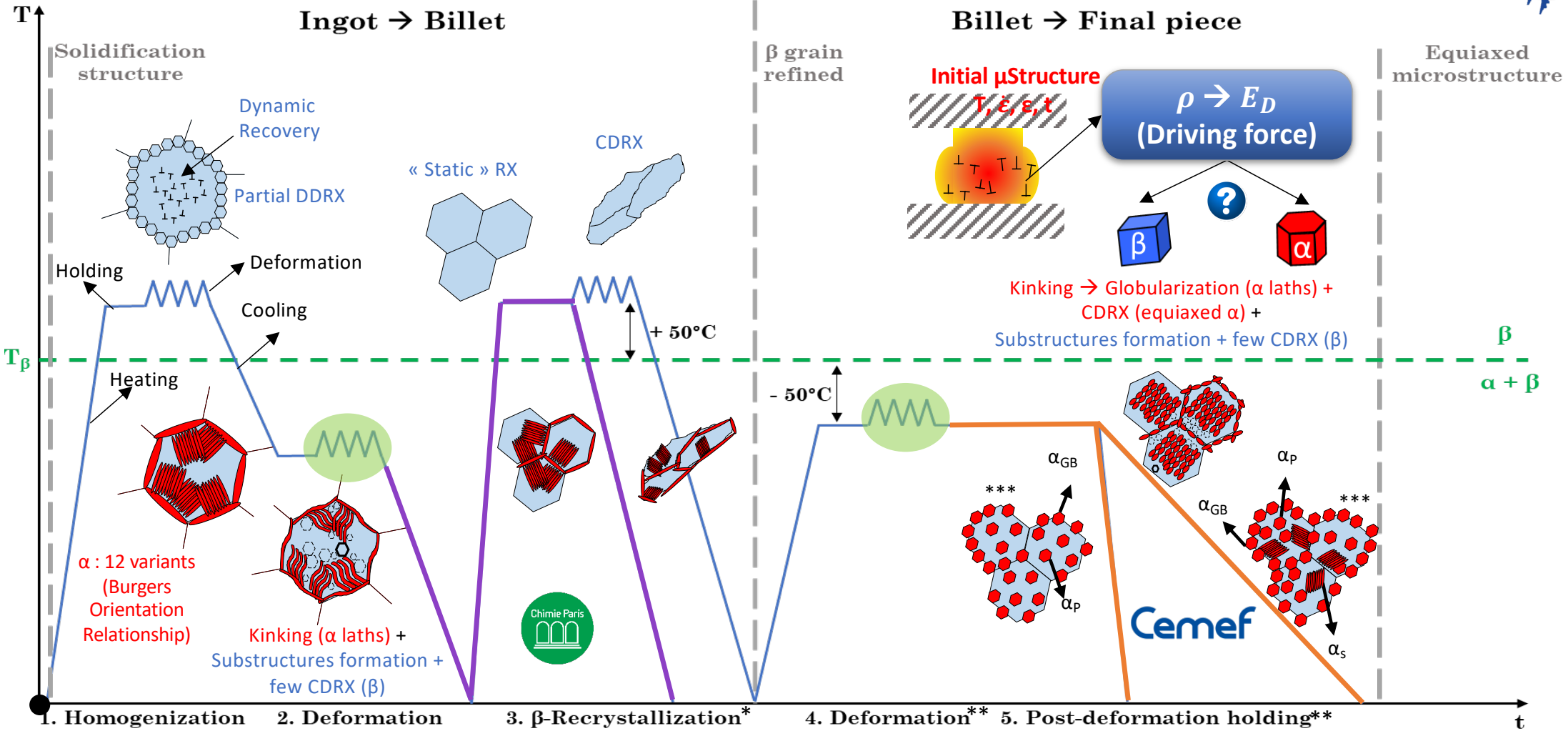

β α

* RX + Def steps repeated several times ** Steps repeated several times *** In the case of cooling β-metastable alloys, for α + β it is rather the reverse

Main objectives

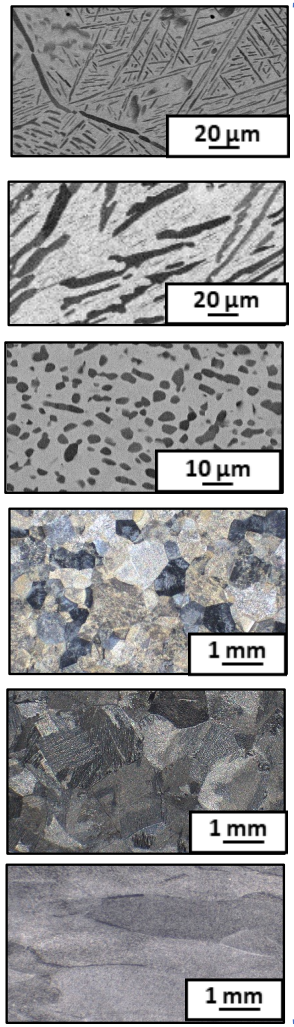

High complexity in the comparison of observed microstructural phenomena in the literature

A vast number of possible microstructures of titanium alloys

Different methods of dislocation density estimation

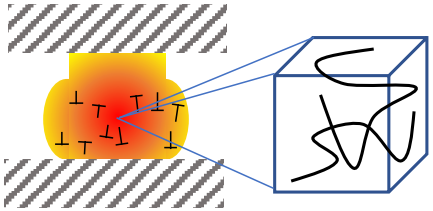

$$\rho\ [m^{-2}] = \frac{L\ [m]}{V[m^3]}$$

3 Approaches

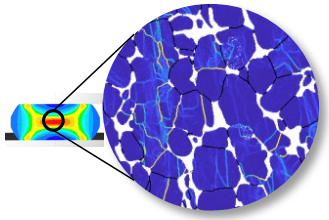

Microscopic Analysis (ρ_{EBSD})

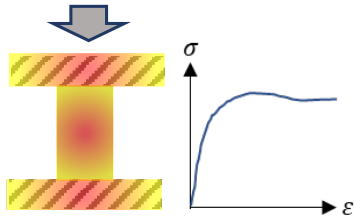

Macroscopic analysis (ρ_{σ})

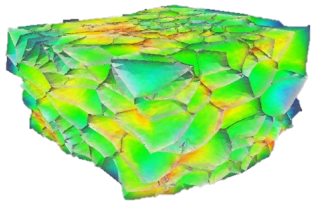

Full field Simulations (ρ_{Sim})

Dislocation densities from different approaches

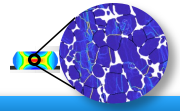

Microscopic Analysis

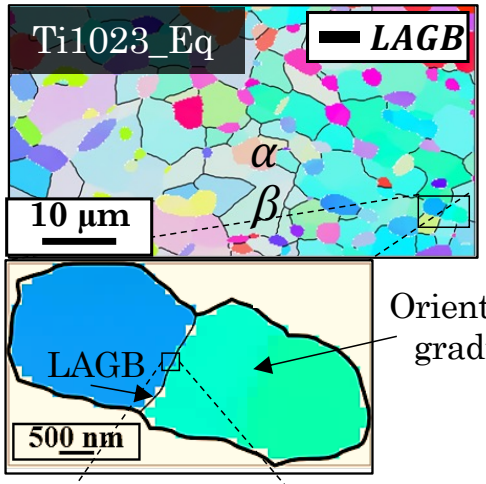

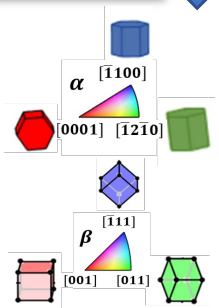

Orientation gradient

Statistically Stored Dislocations (SSD)

ρ_{EBSD} = GND density

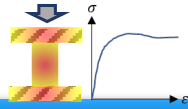

Macroscopic analysis

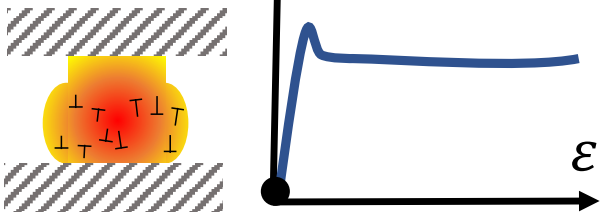

ρ_{σ} = GND + SSD density

Indirect comparison of the 3 approaches

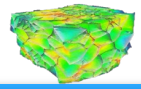

Full field Simulations

Crystal Structure

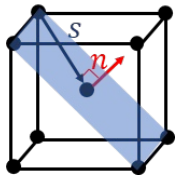

Constitutive models

$$\underline{\dot{\varepsilon}}^{p} = \Psi(\dot{\gamma}^{SS})$$

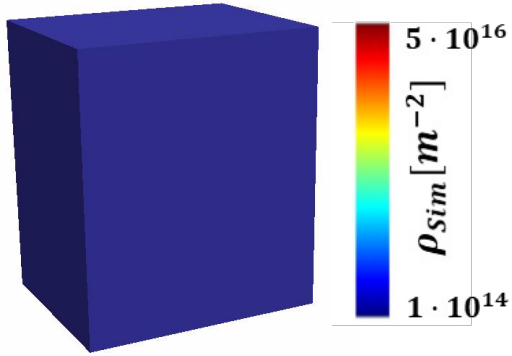

ρ_{Sim} = Strain hardening dislocation density

$$k^{SS} = \Psi(\rho_{Sim})$$

Presentation roadmap

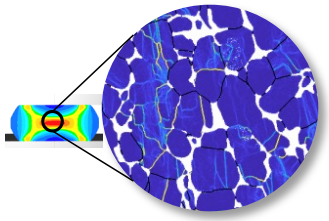

General Introduction + Objectives

Microscopic approach: Microstructural evolution during hot deformation

Macroscopic approach: Rheological analysis based on compression tests

Full field simulation of two-phase microstructure deformation

Conclusions

7 different initial microstructures

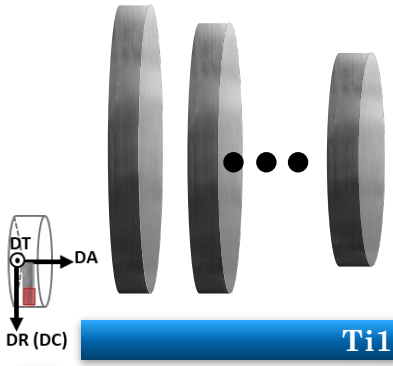

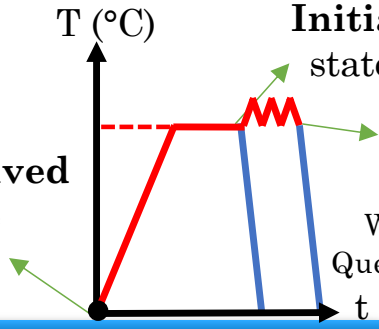

7 initial microstructures (fixed T and $\dot{\varepsilon}$)

4 initial microstructures (Influence of T and $\dot{\varepsilon}$)

T_β - 50°C = 750°C (Ti1023) & 950°C (Ti64)
$\dot{\varepsilon} = 10^{-1}\ s^{-1}$

+ T = 700°C (Ti1023)
+ $\dot{\varepsilon} = 10^{-2}\ s^{-1}$

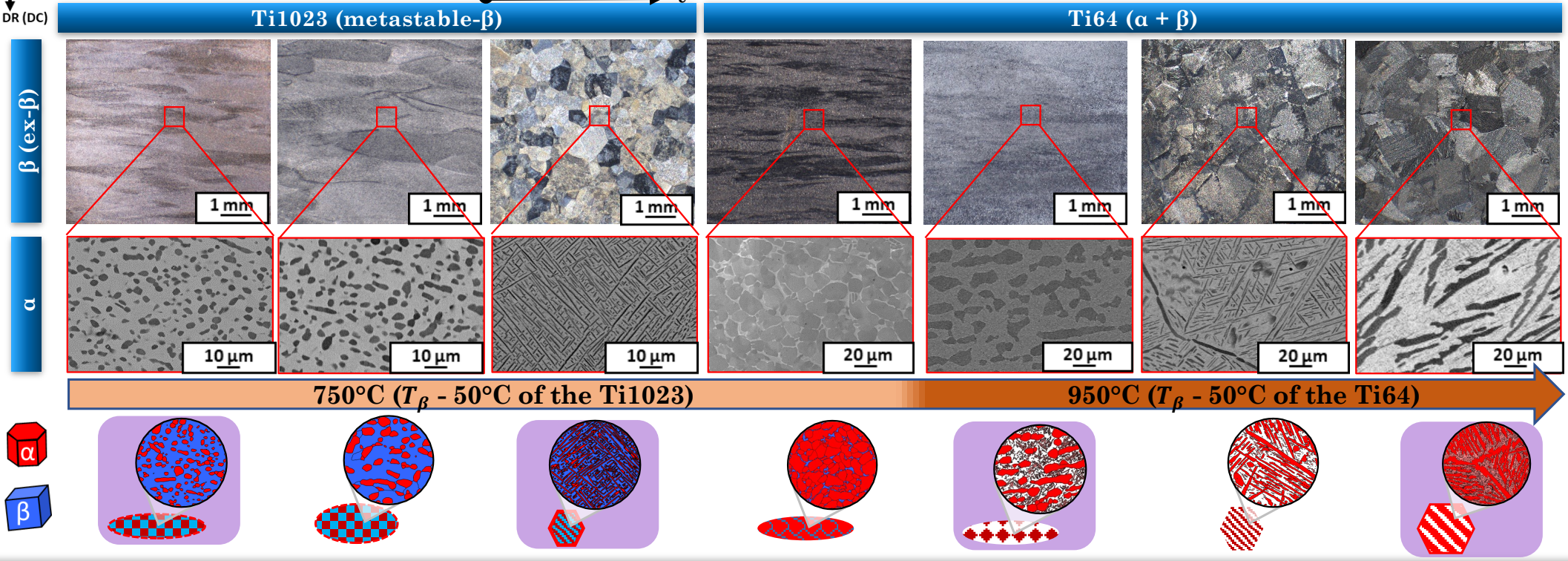

Double-cone samples and EBSD analysis

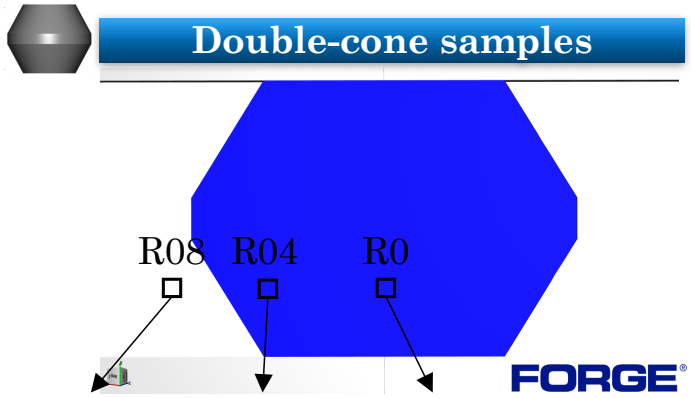

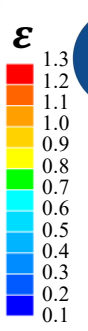

Analyze several strain levels within 1 sample

Several analysis adapted or developped for the different microstructures

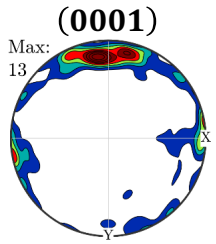

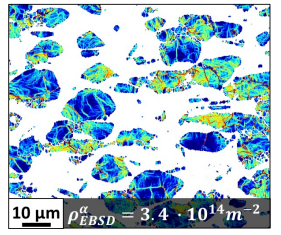

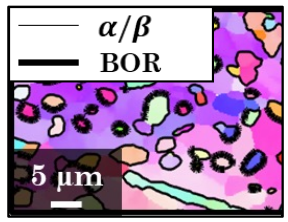

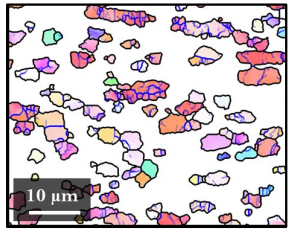

[M. Brozovic Gariglio, N. Bozzolo, and D. Pino Muñoz: Metall. Mater. Trans. A., 2021]

0.3 (0.03 s^{-1}) | 0.8 (0.06 s^{-1}) | 1.3 (0.10 s^{-1})

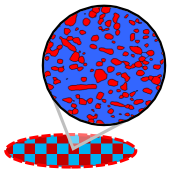

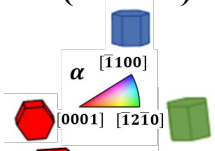

750°C | 10^{-2} s^{-1}

$\varepsilon = 0$ → $\varepsilon = 1.3$

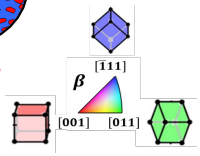

750°C | 10^{-2} s^{-1}

$\varepsilon = 0$ → $\varepsilon = 1.3$

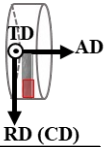

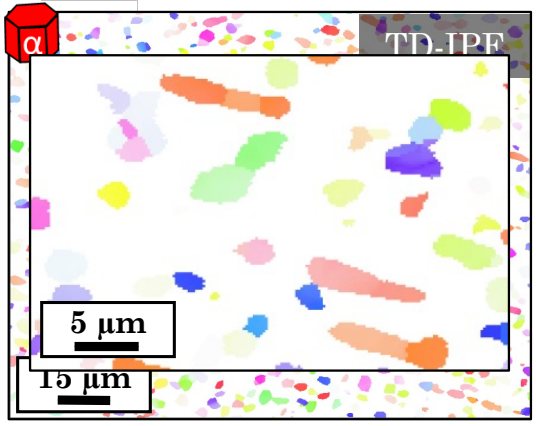

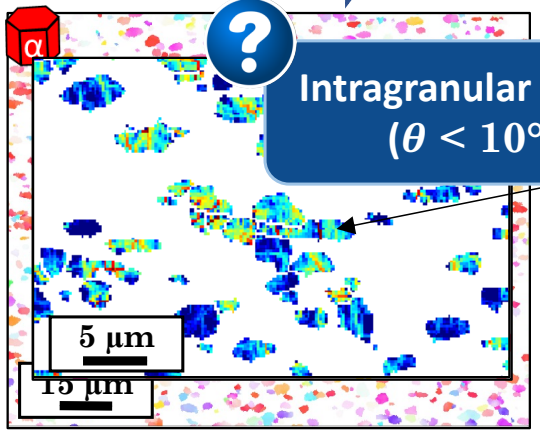

Intragranular misorientations ($\theta < 10°$) → ρ_{EBSD}

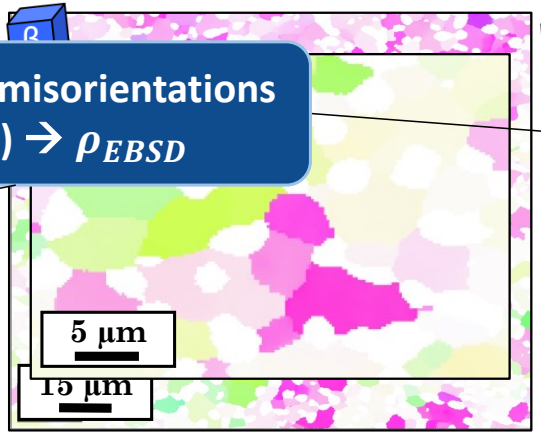

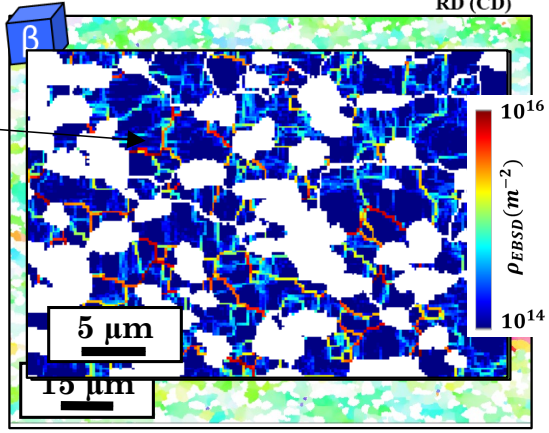

ρ_{EBSD} evolution with increasing deformation (Ti1023 at $T_\beta - 50°C$)

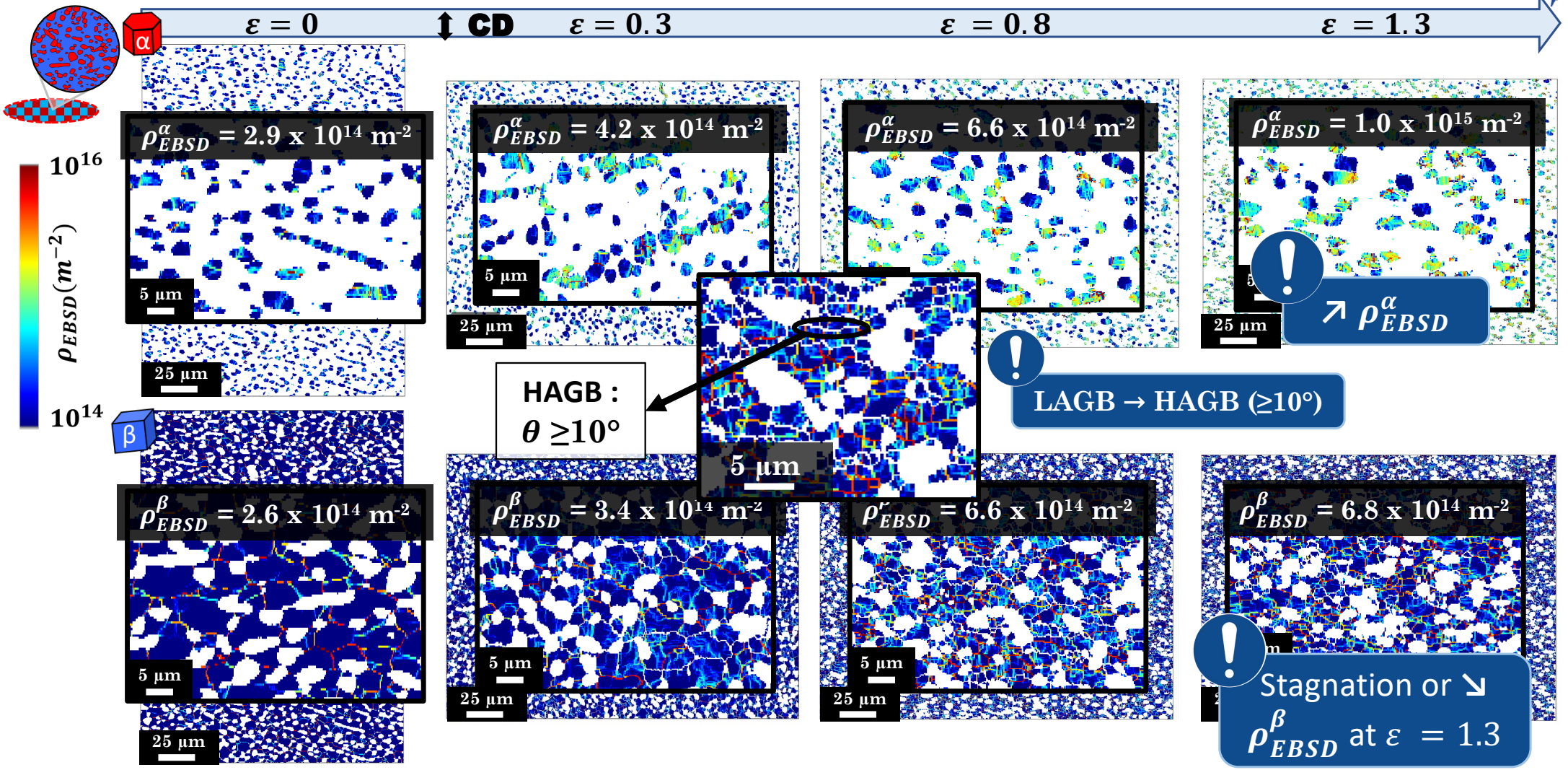

LAGB and HAGB density

Phase maps + LAGB and HAGB

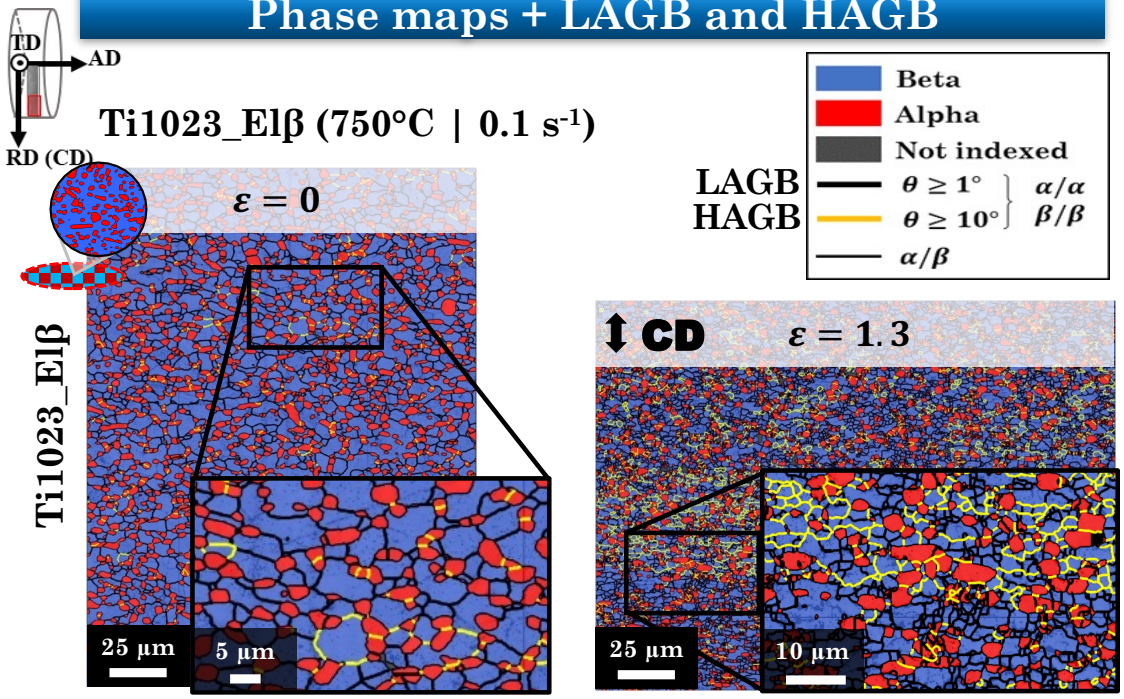

Cumulative analysis of $\rho_{LAGB} + \rho_{HAGB}$

$$\rho_{GB}(\geq \theta)[\mu m^{-1}] = \frac{Grain\ Boundary\ Length\ (\geq \theta)\ [\mu m]}{Grain\ area\ [\mu m^2]}$$

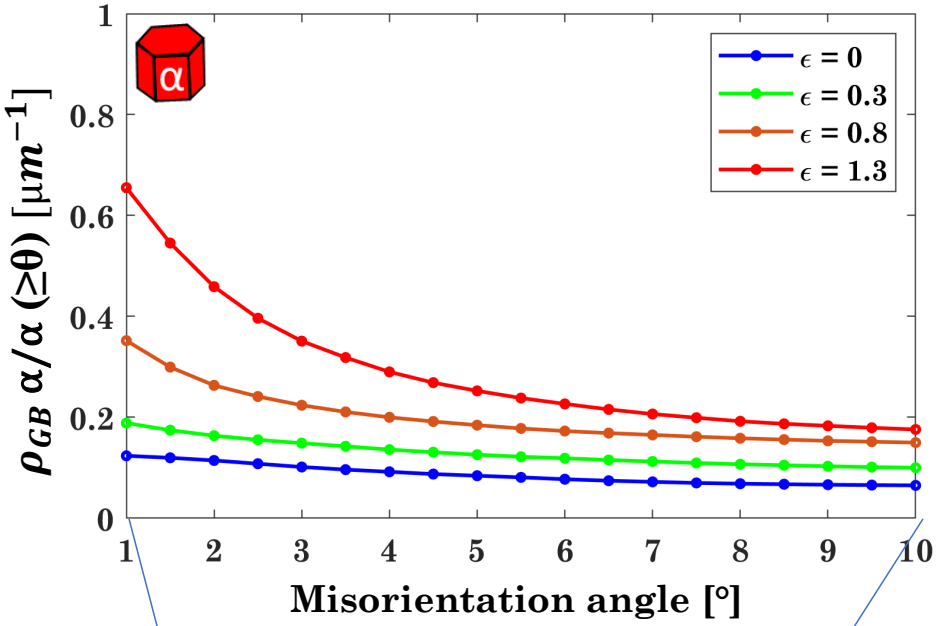

$\rho_{GB}\ (\geq 1°) = \rho_{LAGB} + \rho_{HAGB}$

$\rho_{HAGB}\ (\geq 10°)$

LAGB and HAGB density for **equiaxed** Ti1023

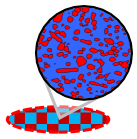

α

β

$700°C \mid 10^{-2}s^{-1}$ ↗ T $750°C \mid 10^{-2}s^{-1}$ ↗ $\dot{\varepsilon}$ $750°C \mid 10^{-1}s^{-1}$

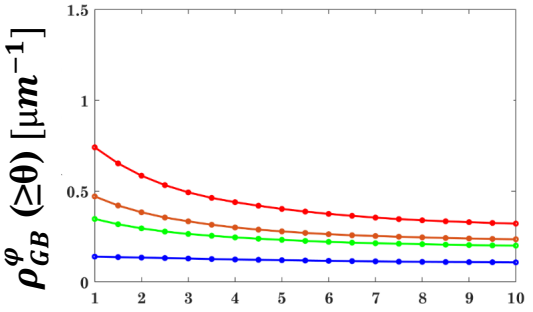

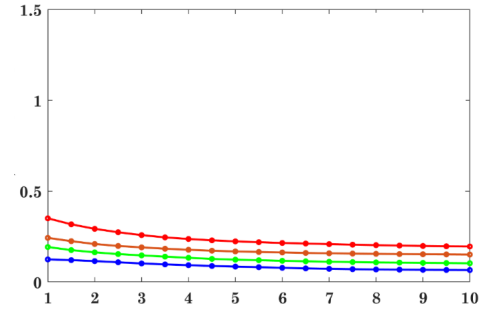

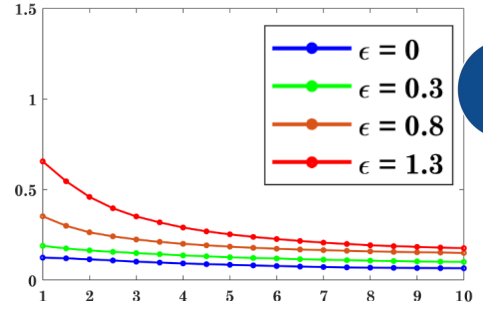

↗ T = ↘ ρ_{LAGB}^{α}
↗ $\dot{\varepsilon}$ = ↗ ρ_{LAGB}^{α}

CD

$\varepsilon = 1.3$

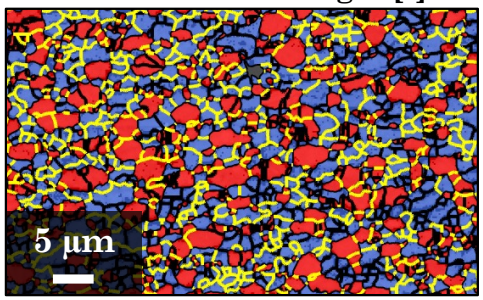

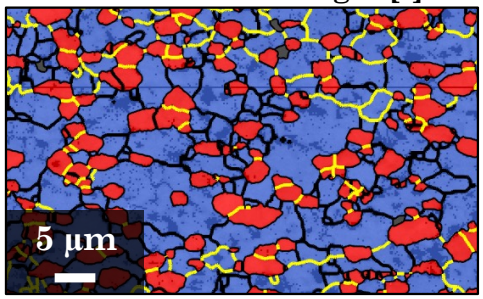

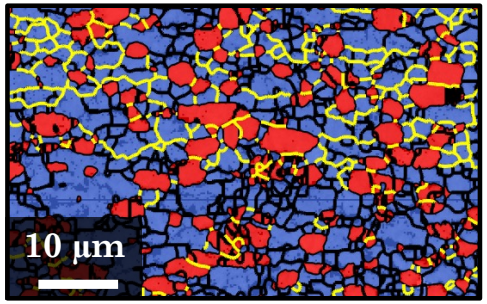

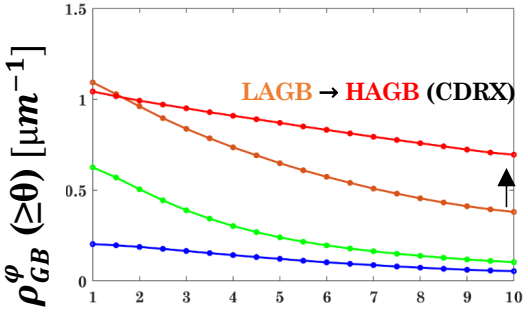

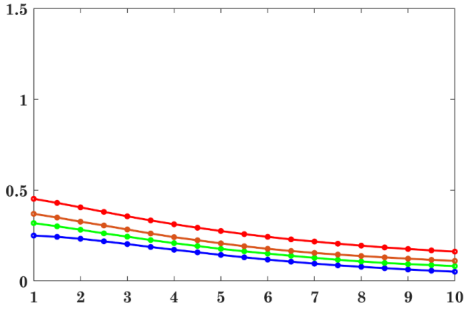

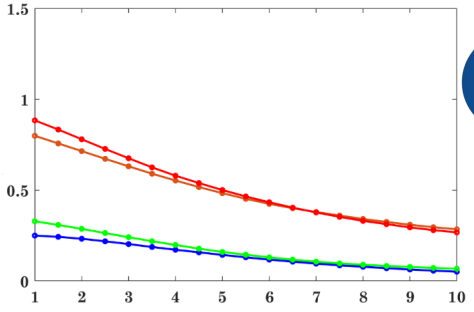

↗ T = ↘ ρ_{GB}^{β}
↗ $\dot{\varepsilon}$ = ↗ ρ_{GB}^{β}

LAGB and HAGB density for **lamellar** Ti1023

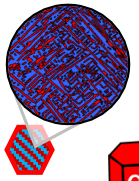

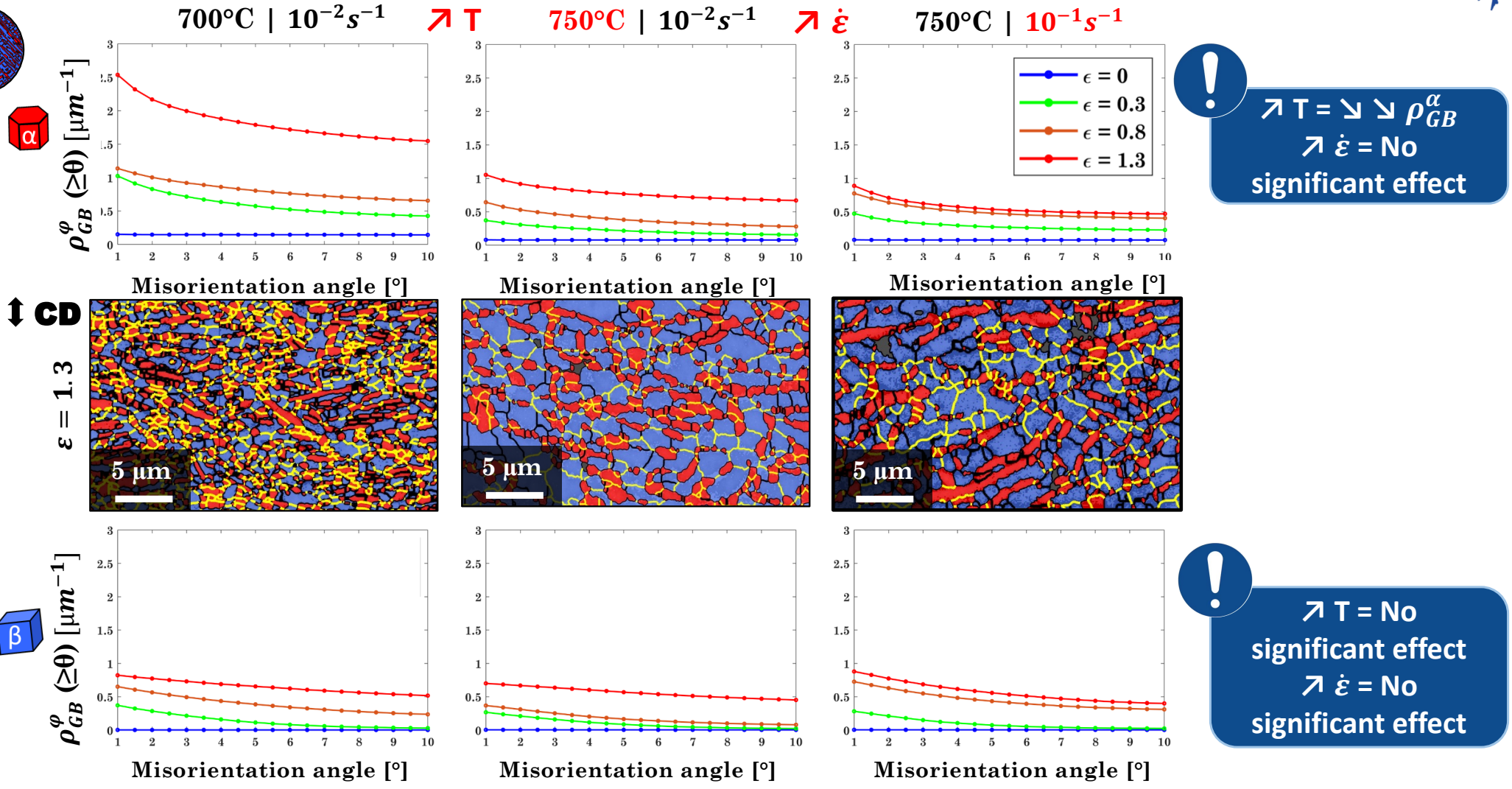

↗ T = ↘ ↘ ρ_{GB}^{α}
↗ $\dot{\varepsilon}$ = No significant effect

↗ T = No significant effect
↗ $\dot{\varepsilon}$ = No significant effect

Trends in the microstructural evolution of the α phase (T_β - 50°C | 0.1 [illegible])

Equiaxed α / Elongated β

Lamellar α / Equiaxed β

Ti1023

µStructures	α Morphology	α Texture (local)	α TD-IPF at ε = 1.3	ρ_{LAGB} in α grains

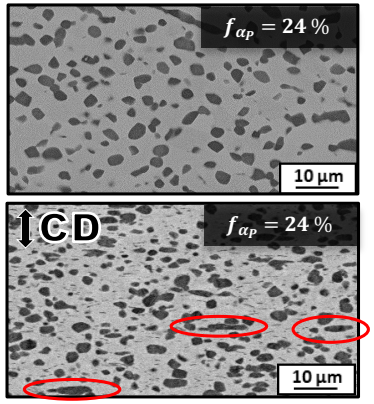

Alignment of elongated α nodules

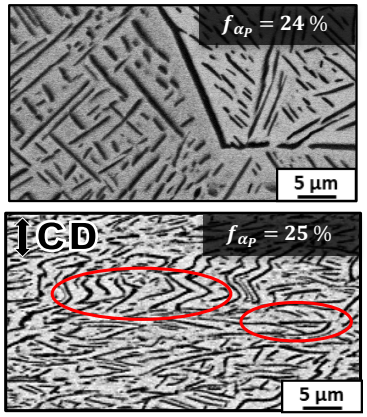

Kinking, breakage and alignment of the α laths

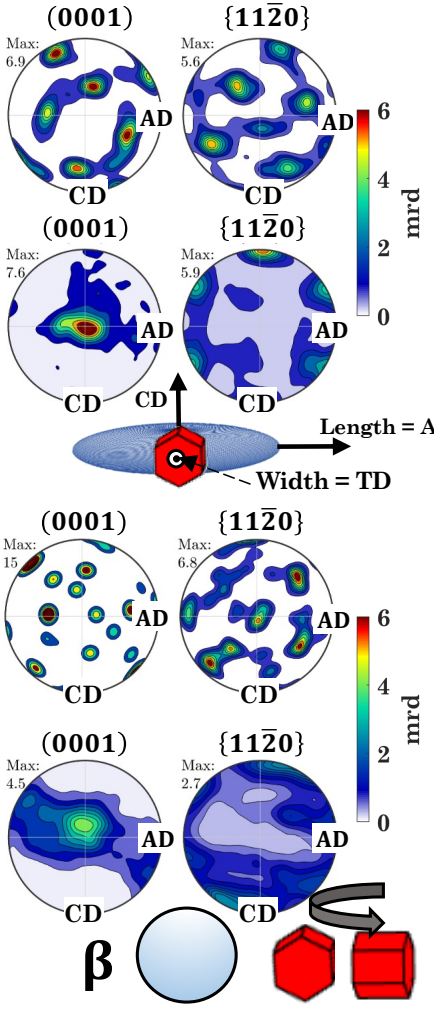

Highly elongated grains

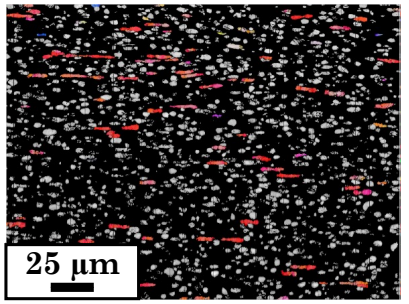

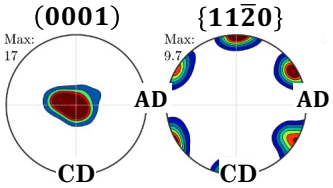

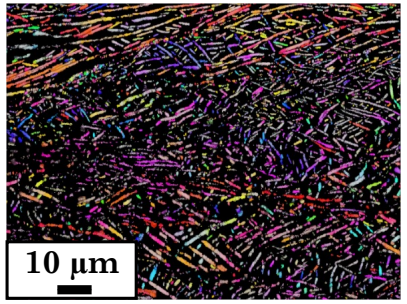

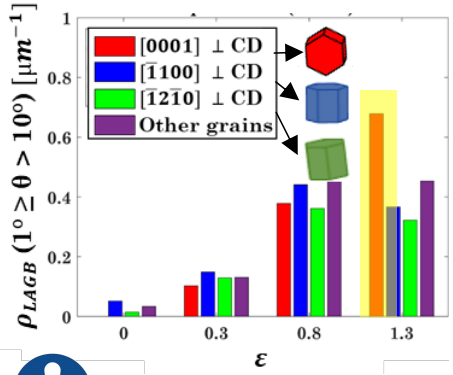

↗ ρ_{LAGB} (formation of substructures) within grains respecting this specific developed orientation

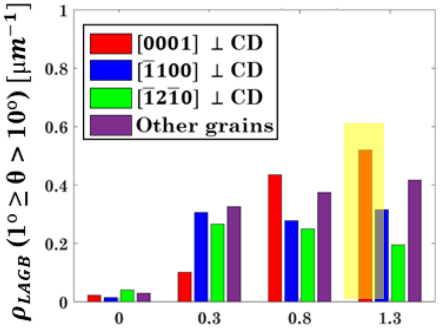

Behaviors also valid for the Ti64 microstructures

α local texture trend also observed for different T and $\dot{\varepsilon}$ tested

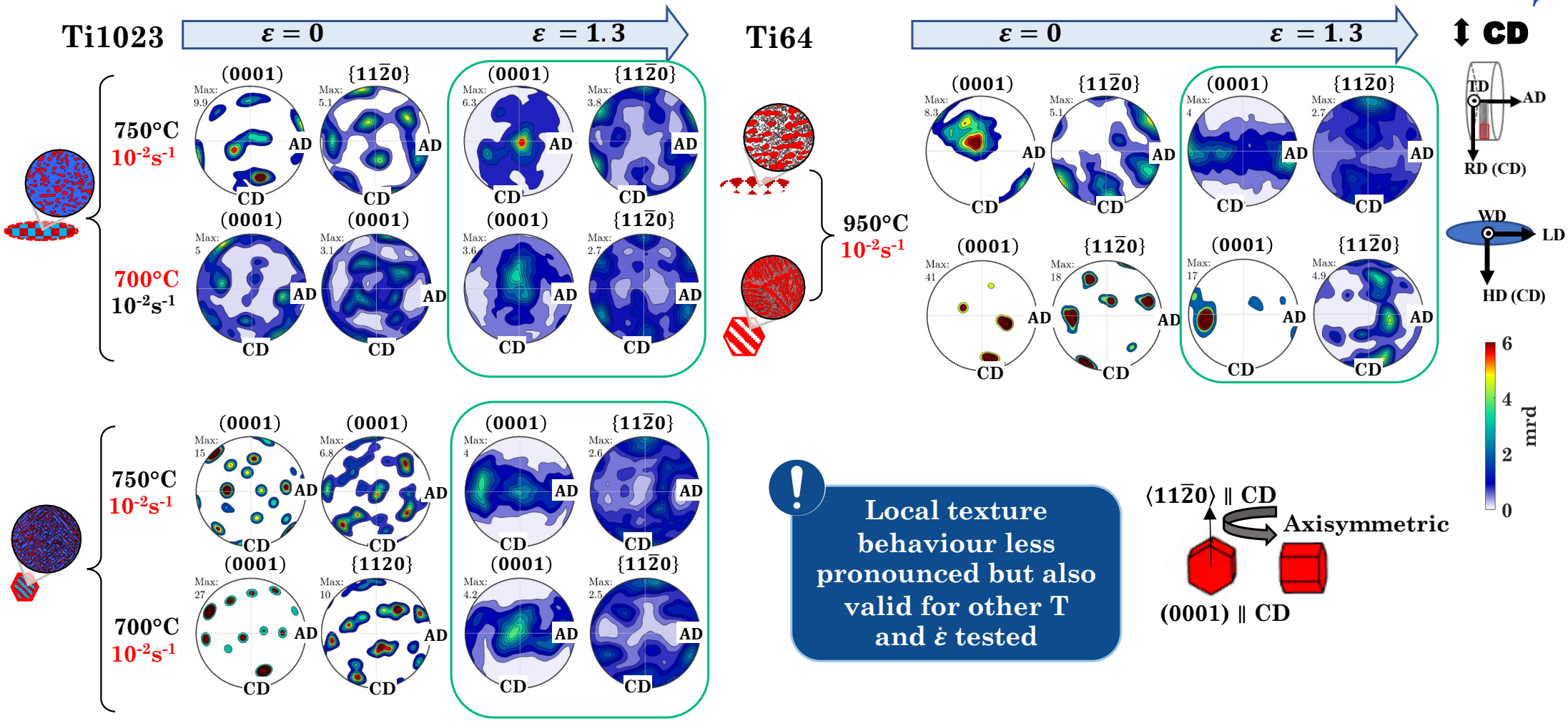

Orientation dependency of ρ_{LAGB} in α grains for different T and $\dot{\varepsilon}$ tested

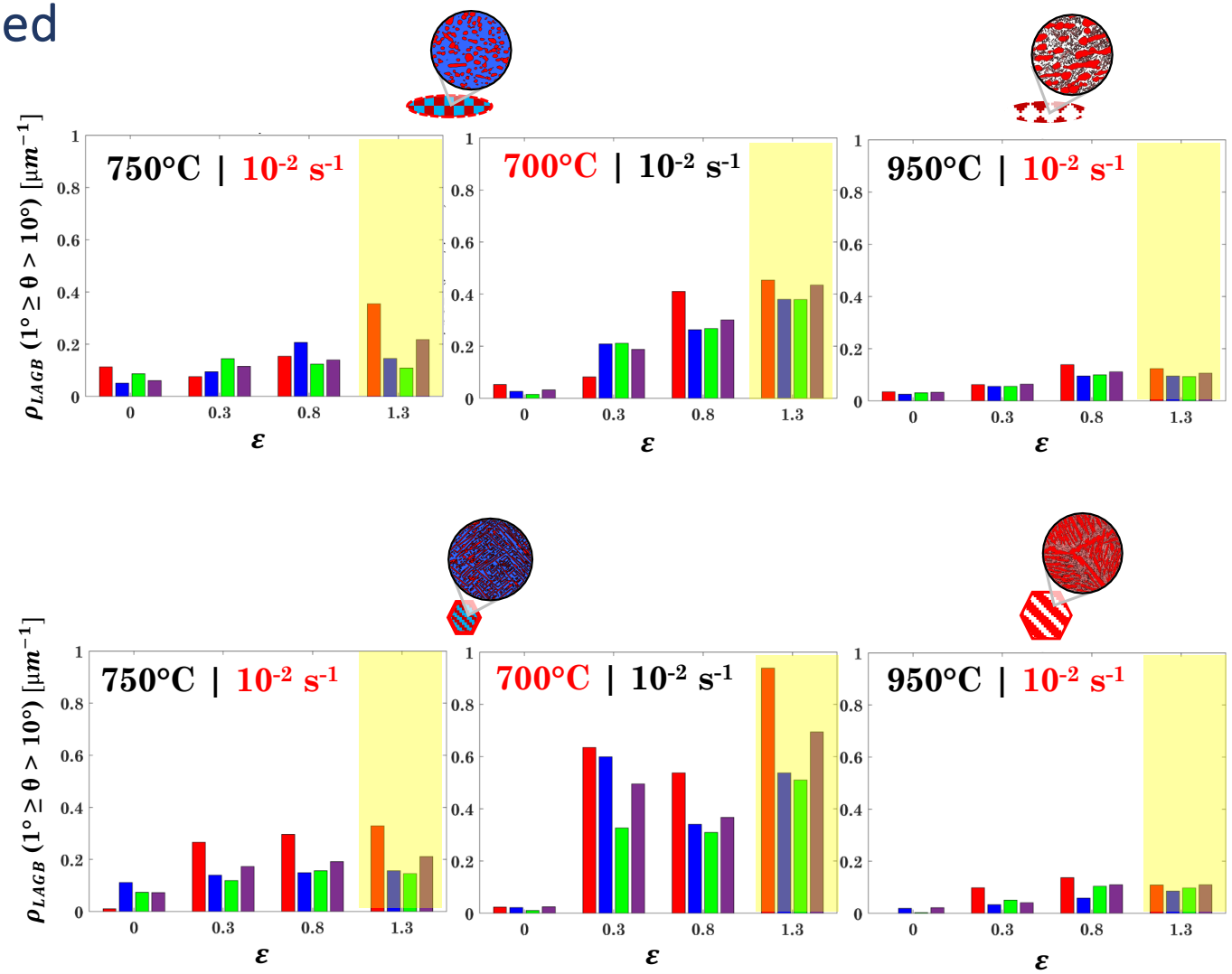

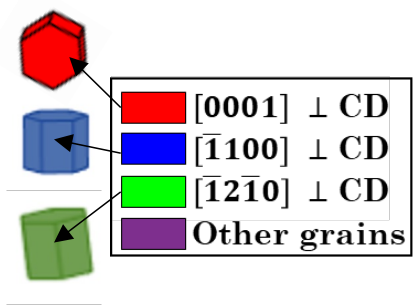

↗ ρ_{LAGB} (1° ≥ θ > 10°)

Identification of an intrinsic behavior of the α phase

Presentation roadmap

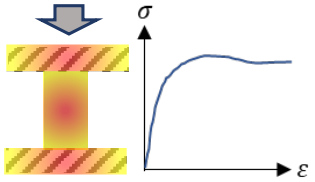

General Introduction + Objectives

Microscopic approach: Microstructural evolution during hot deformation

Macroscopic approach: Rheological analysis based on compression tests

Full field simulation of two-phase microstructure deformation

Conclusions

+ Comparison with Microscopic approach

How to assess the σ_α & σ_β

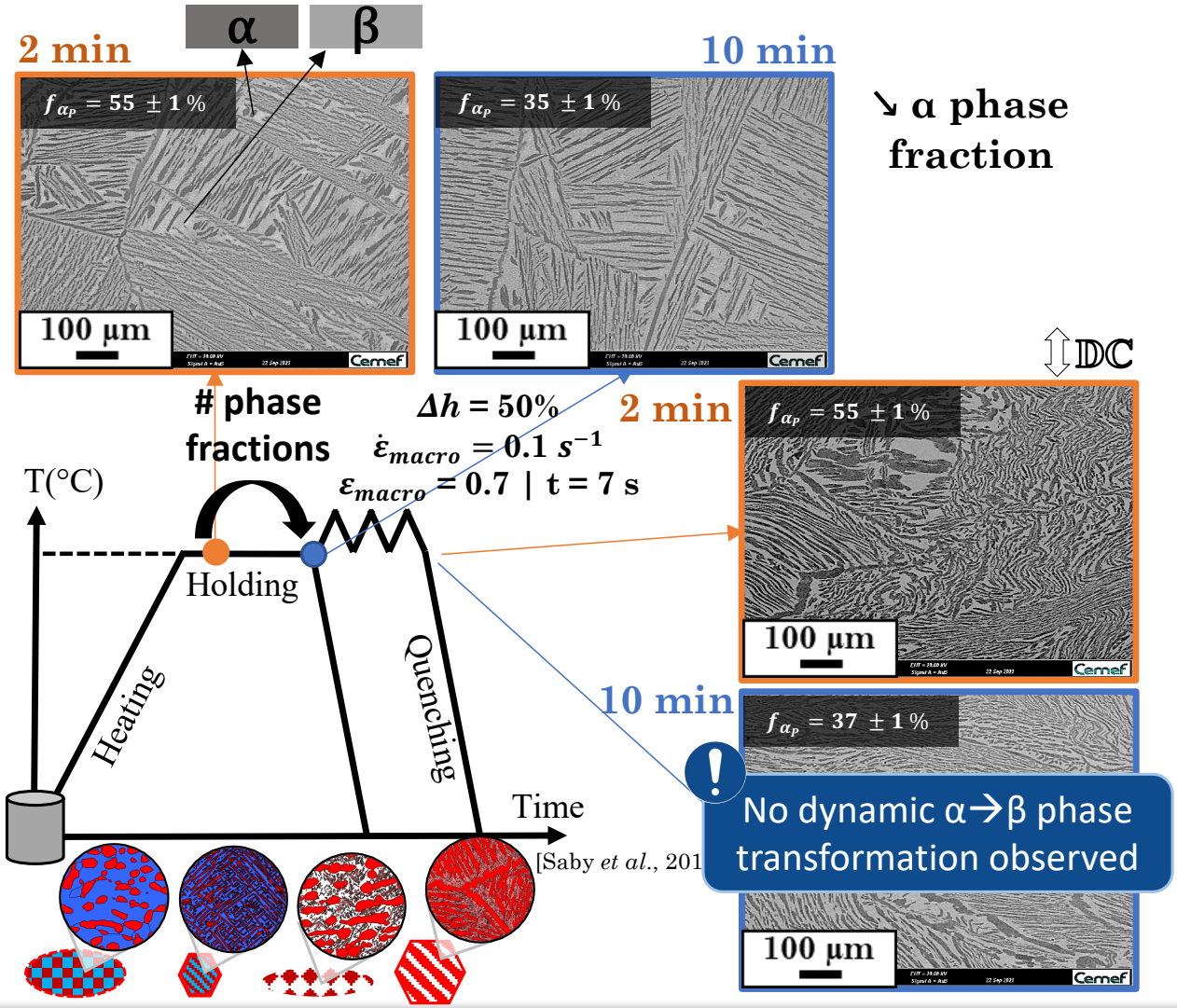

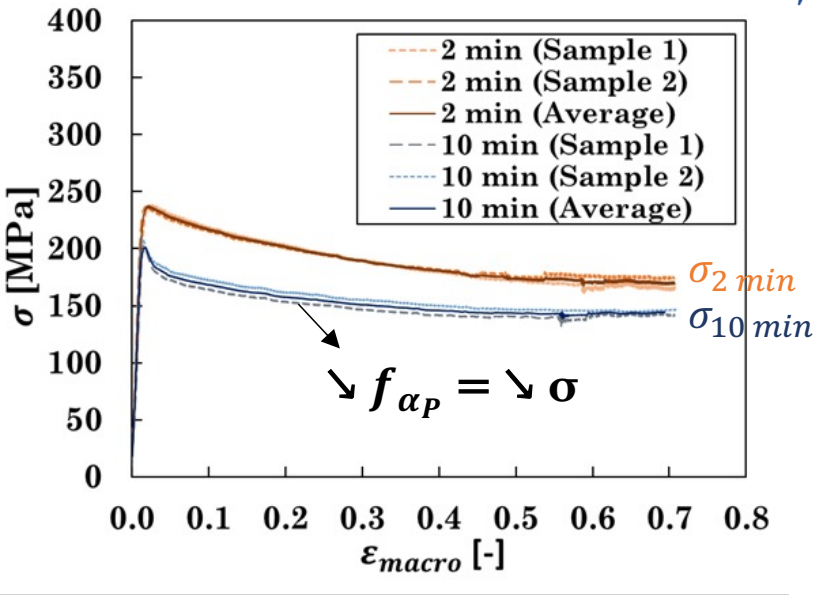

Rule of Mixtures
(Voigt assumption)

$$\sigma_{2\,min} = \sigma_\alpha f_\alpha + \sigma_\beta (1 - f_\alpha)$$
$$\sigma_{10\,min} = \sigma_\alpha f_\alpha + \sigma_\beta (1 - f_\alpha)$$

$f_{\alpha_P} \approx$ constant throughout the compression

Stress-strain curves analysis for the 4 initial microstructures

Ti64 | 950°C | 0.1s^{-1}

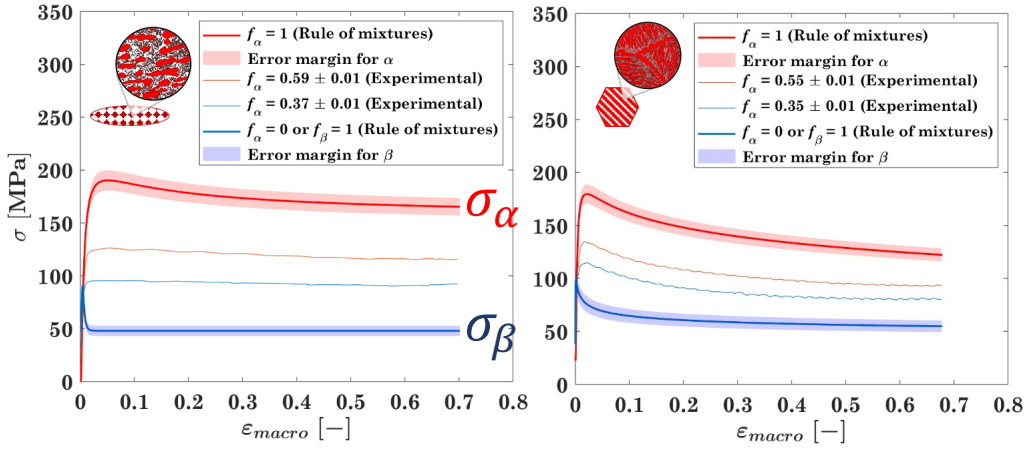

Ti1023 | 750°C | 0.1s^{-1}

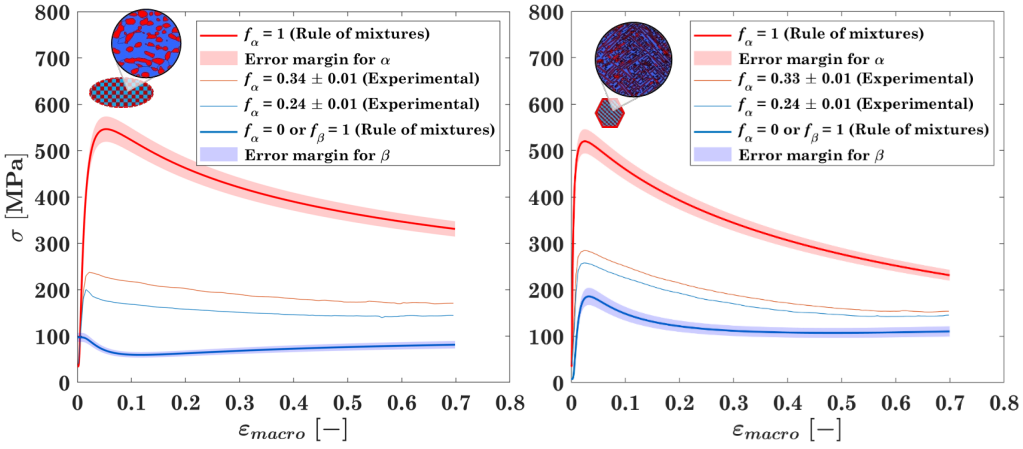

Softening on the **experimental curves** (orange and light blue)
→ Related to the **α phase**

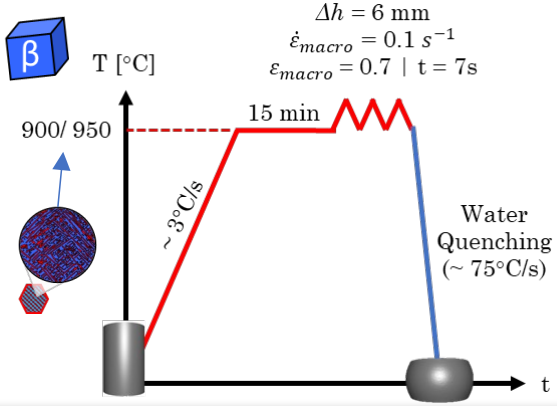

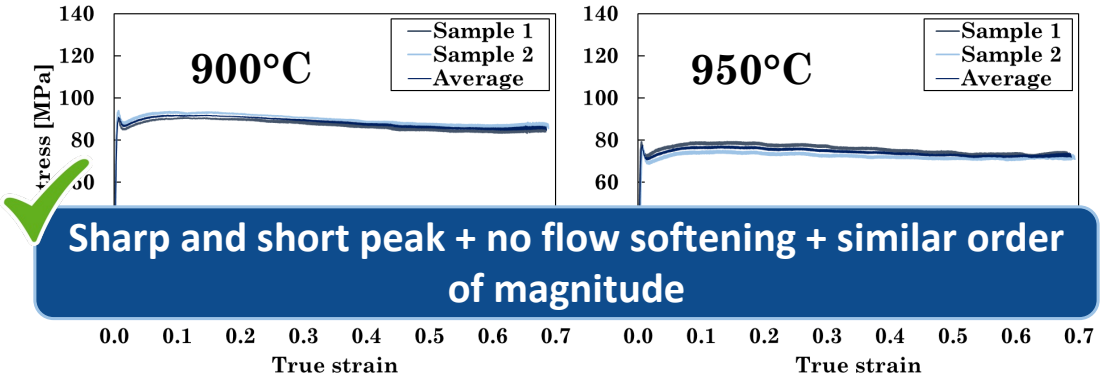

Sharp and short peak + no flow softening + similar order of magnitude

$$\sigma_\varphi = \sigma_0 + \psi M_\varphi G_\varphi b_\varphi \sqrt{\rho_\sigma^\varphi}$$

[Buzolin et al., International Journal of Plasticity, 2021 ;
M. Semblanet (PhD thesis), 2014]

Comparison between Micro and Macro methods for the Ti1023 (α)

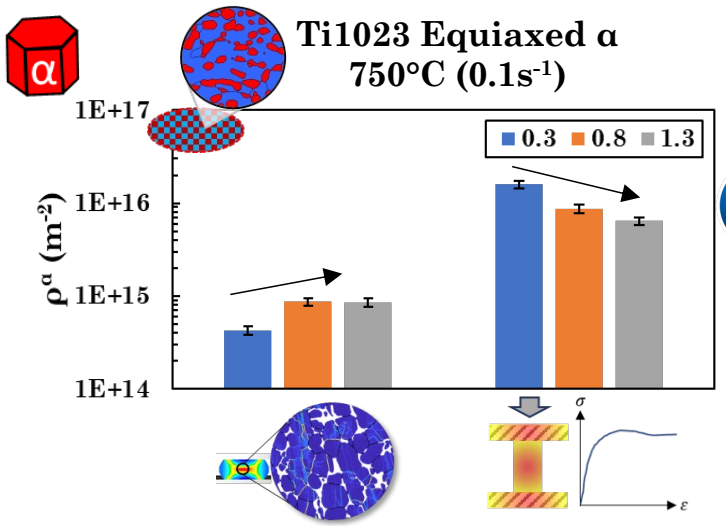

Different behaviors

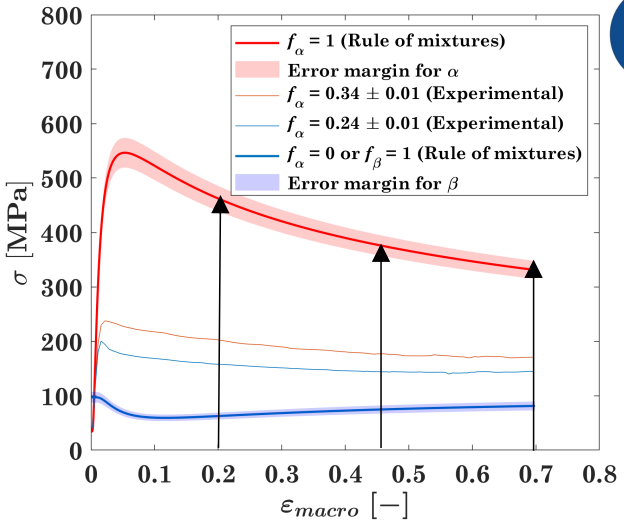

Flow softening : α grains elongation + alignment ⊥ CD + texture development to softer configuration

[Semiatin, MMTA, 2020]

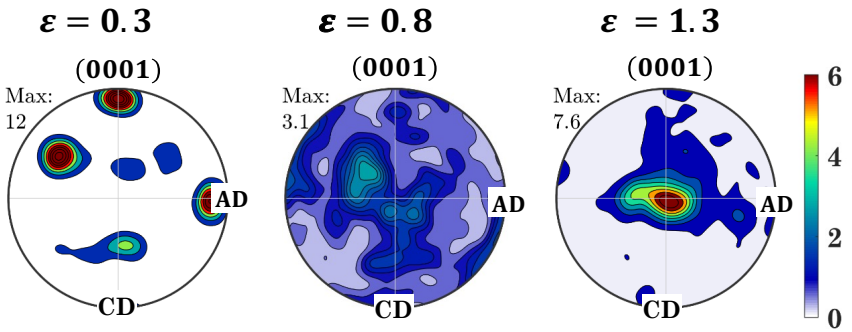

Strong crystallographic texture at ε = 1.3

Normal of Basal plane perpendicular to the compression axis [0001] ⊥ CD

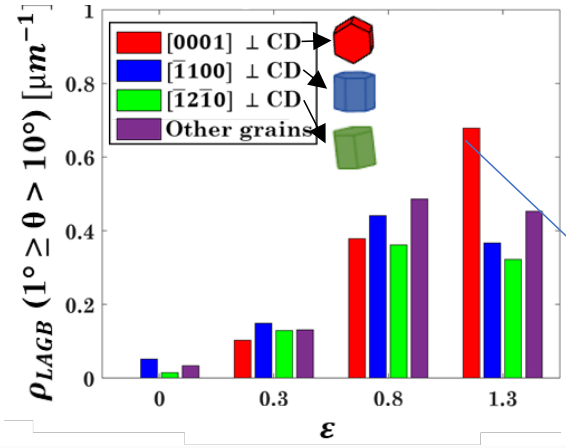

α grains [0001] ⊥ CD : ↗ ρ_{LAGB}

Confrontation between Micro and Macro methods for the Ti64 (α)

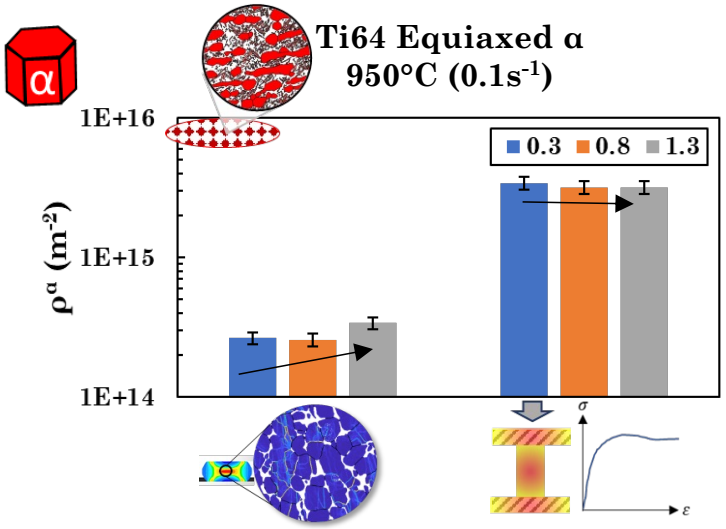

Almost no ↘ ρ_σ

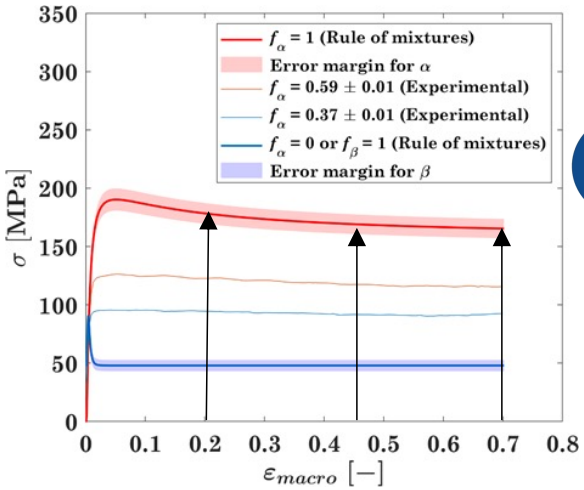

Very slight flow softening

$\varepsilon = 0.3$ $\varepsilon = 0.8$ $\varepsilon = 1.3$

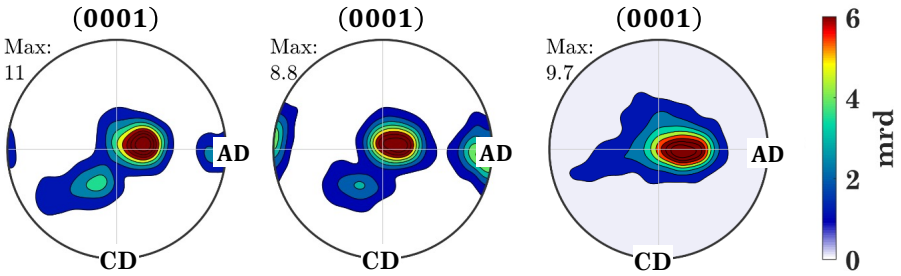

Strong texture already observed at $\varepsilon = 0.3$

Basal plane parallel to the compression axis
[0001] ⊥ CD

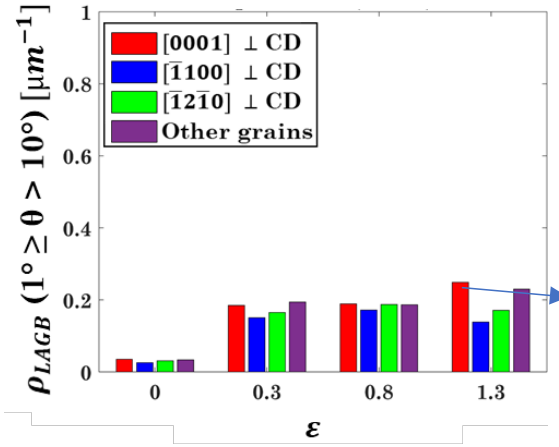

α grains [0001] ⊥ CD : ↗ ρ_{LAGB}

Confrontation between Micro and Macro methods for the Ti1023 (β)

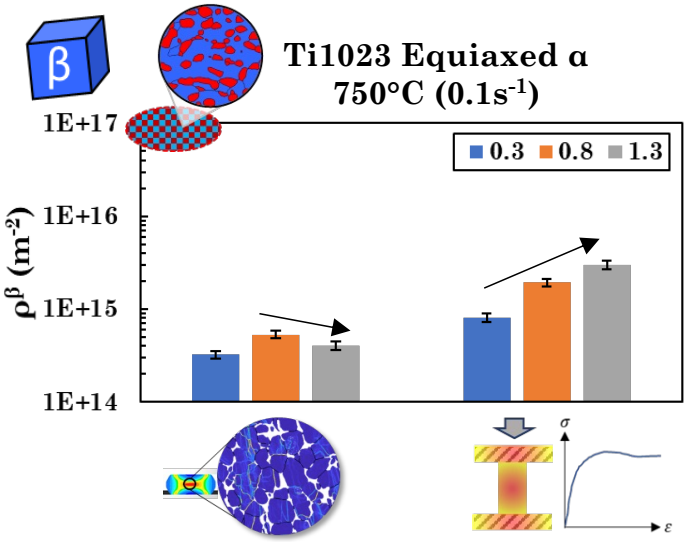

Different behaviors

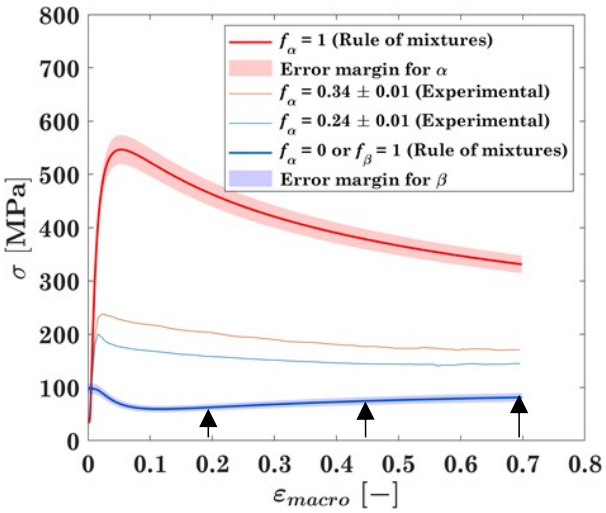

CDRX : ↗ ρ_σ, ↘ average grain size, ↗ σ

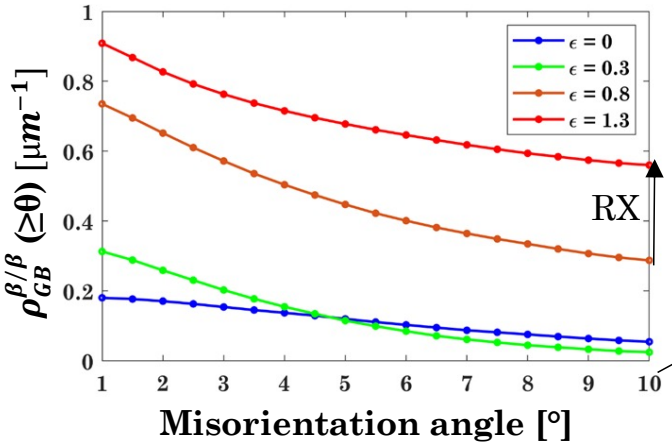

10° → Threshold for the ρ_{EBSD} analysis

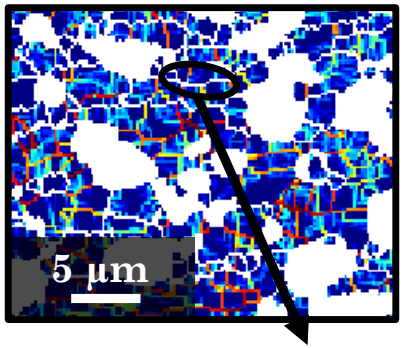

$\theta \geq 10°$

↘ ρ_{EBSD} (0.8 ≤ ε ≤ 1.3) = CDRX (LAGB → HAGB)

Presentation roadmap

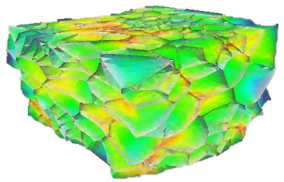

General Introduction + Objectives

Microscopic approach: Microstructural evolution during hot deformation

Macroscopic approach: Rheological analysis based on compression tests

Full field simulation of two-phase microstructure deformation

Conclusions

1st step towards more realistic simulations

How to perform crystal plasticity finite element method simulations

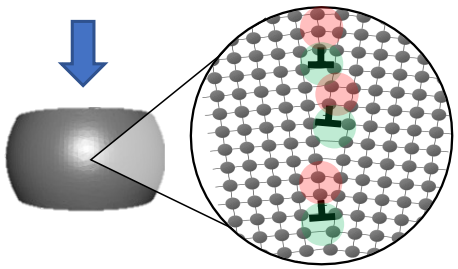

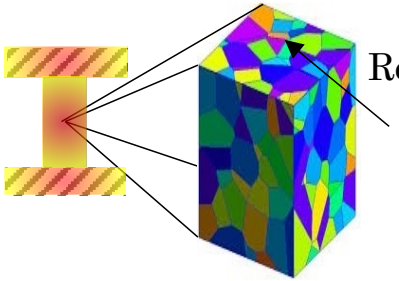

Representative Volume Element (RVE)

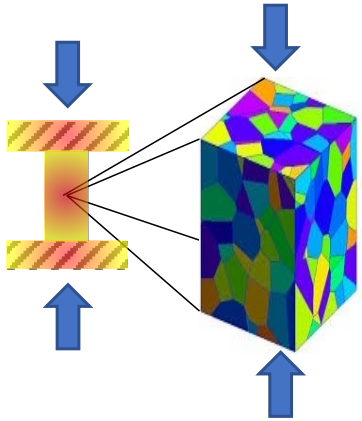

Crystal plasticity model

Computational domain (inside one β grain)

Boundary Conditions

Trends in the dislocation density estimation from simulations → ρ_{Sim}

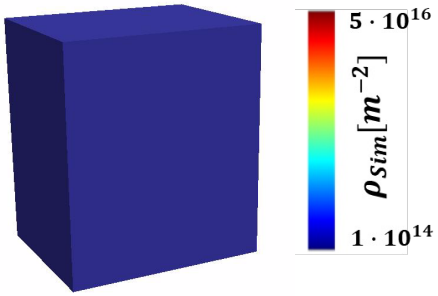

Dislocation density analysis and comparison with the EBSD data

ρ_{Sim} for equiaxed case
(orientations from 2D EBSD)

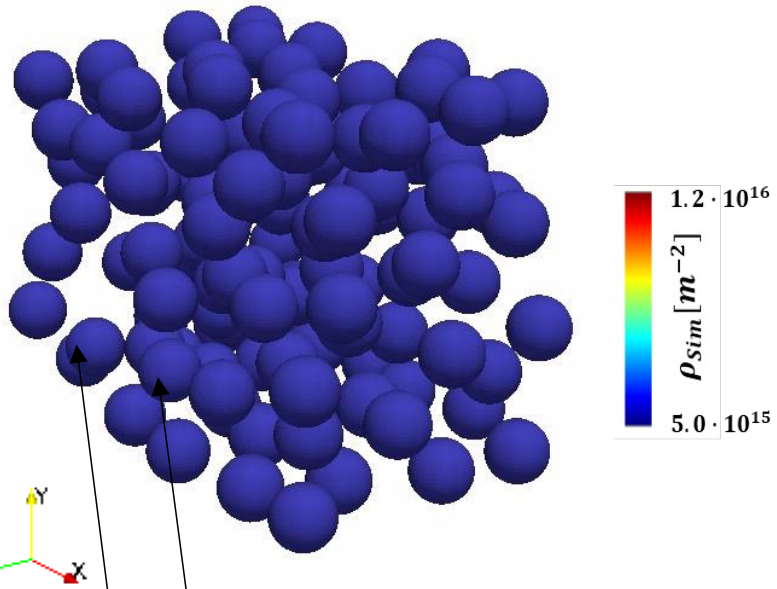

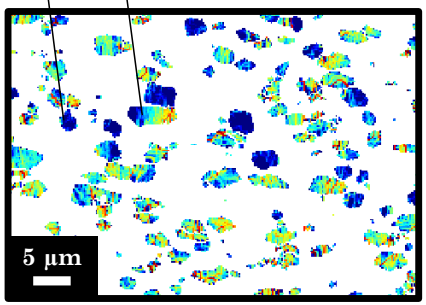

ρ_{Sim} for lamellar case
(orientations from 3D EBSD)

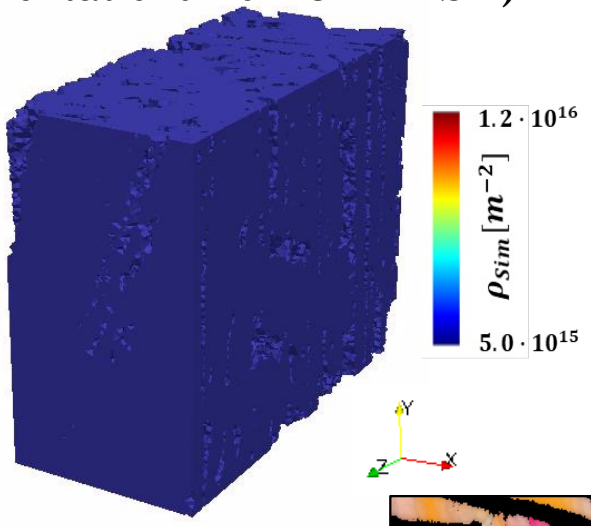

2D EBSD

Orientations

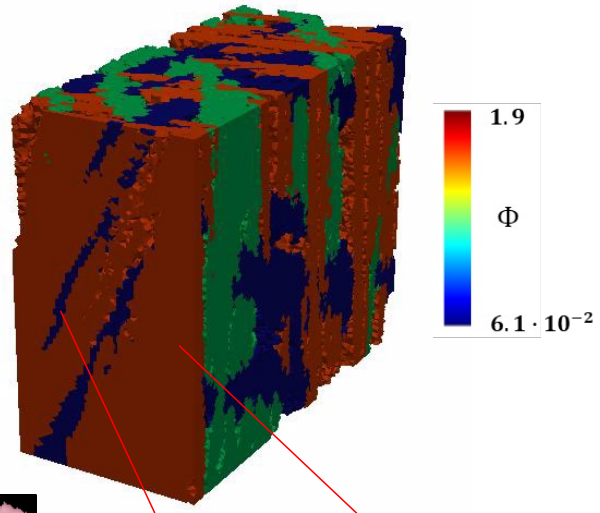

α grain orientation influence

Simulation *vs* Experiments → similar trends

Kinking

Orientation gradient

Presentation roadmap

General Introduction + Objectives

Microscopic approach: Microstructural evolution during hot deformation

Macroscopic approach: Rheological analysis based on compression tests

Full field simulation of two-phase microstructure deformation

Conclusions

Conclusions on the comparison of 3 approaches

3 approaches to **estimate** dislocation densities → **not directly measured**

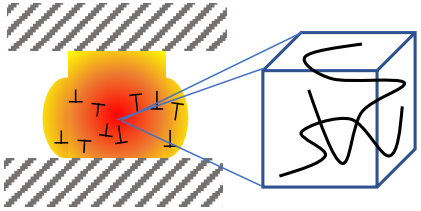

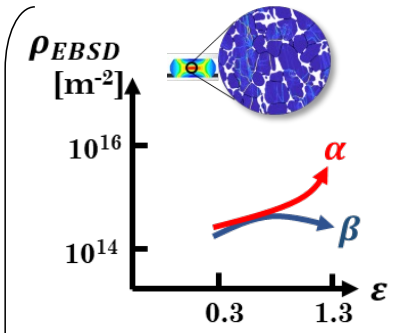

α **Crystallographic texture : (0001) and ⟨11$\bar{2}$0⟩ ∥ CD → ↗ ρ_{LAGB}**

β **CDRX at ↗ ε → HAGB not accounted in the model + ↘ ρ_{LAGB} inside the new grains.**

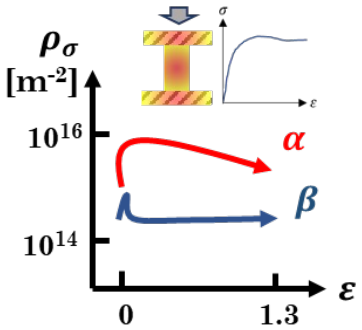

α **Crystallographic texture : (0001) and ⟨11$\bar{2}$0⟩ ∥ CD → softer configuration (flow softening)**

β **CDRX**

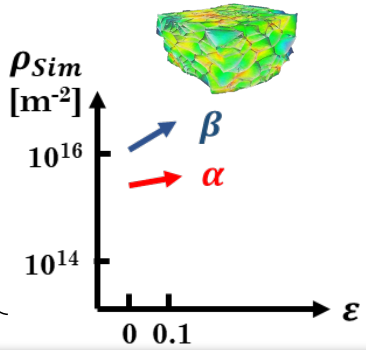

α **Crystallographic orientation dependency**

β **↘ CRSS and G values + single grain in the RVE**

Conclusions on the microstructural evolution of titanium alloys

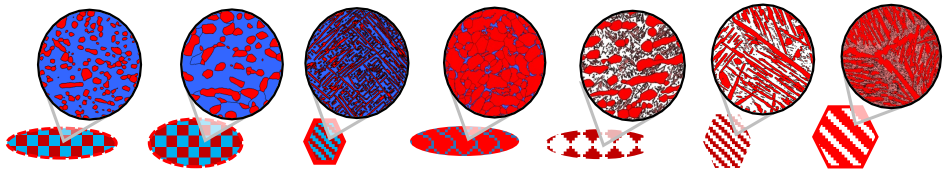

Identification of an intrinsic behavior of the α phase
$T_\beta - 50°C$ et $T_\beta - 100°C$ + 10^{-2} s^{-1} et 10^{-1} s^{-1}

Before deformation

Morphological alignment ⊥ CD

Equiaxed

Lamellar

↕CD

$\varepsilon = 1.3$

Elongation of equiaxed α grains with a specific orientation

Crystallographic orientation with $\langle 11\bar{2}0 \rangle$ ∥ CD and Basal Plane ∥ CD

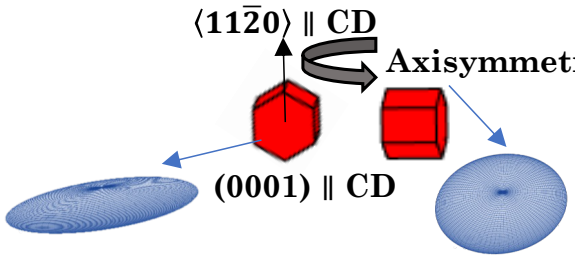

The formation of substructures accompanies the change in orientation and morphology

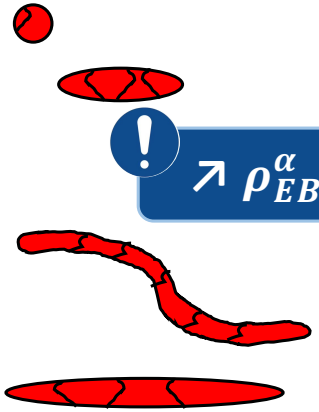

↗ ρ^{α}_{EBSD}

Identification of the influence of the initial microstructure, T and $\dot{\varepsilon}$ on the α and β phase evolutions

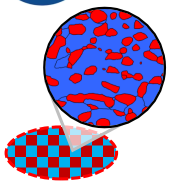

↗ ρ^{φ}_{GB}

α **↘ T + ↗ $\dot{\varepsilon}$ (Mostly LAGB)**

β **↘ T + ↗ $\dot{\varepsilon}$**

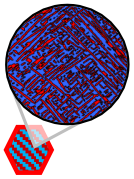

↗ ρ^{φ}_{GB}

α **↘ T (Strong effect)**

β **No significant effect**

Thank you for your attention!

Matheus BROZOVIC GARIGLIO

matheus.brozovic-gariglio@safrangroup.com

Perspectives

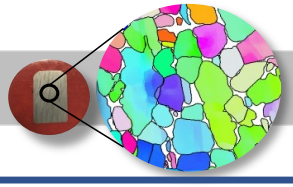
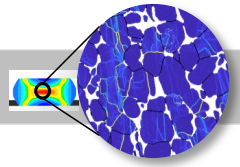
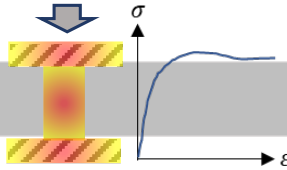

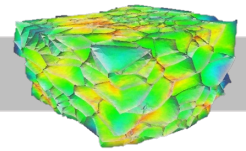

Influence of Cooling rate

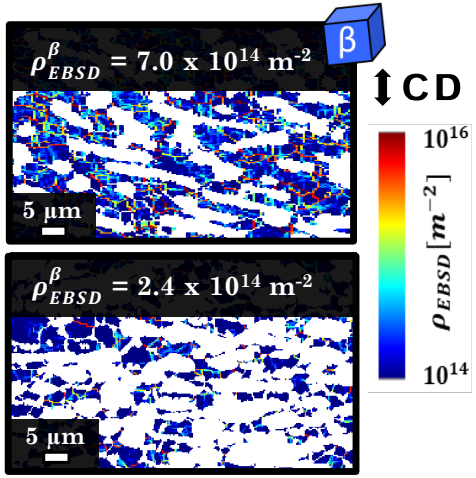

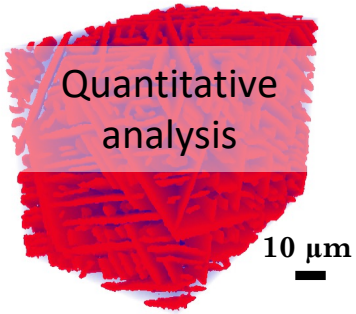

Ti64 at 750°C

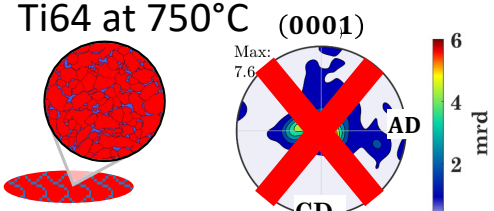

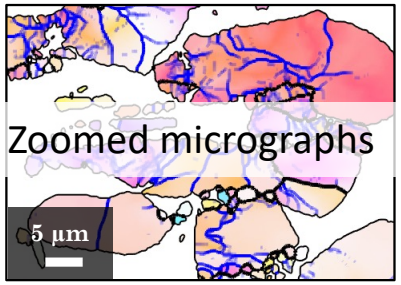

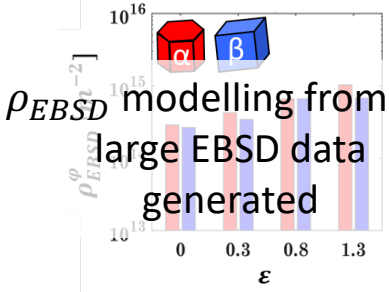

ρ_{EBSD} modelling from the large EBSD data generated

Improve ROM through other $\dot{\varepsilon}$, T (10^{-2} s^{-1} and 700°C)

$$\sigma = \sigma_\alpha f_\alpha + \sigma_\beta (1 - f_\alpha)$$
$$\sigma = \sigma_\alpha f_\alpha + \sigma_\beta (1 - f_\alpha)$$

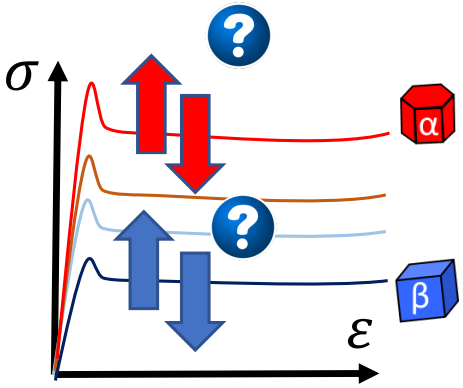

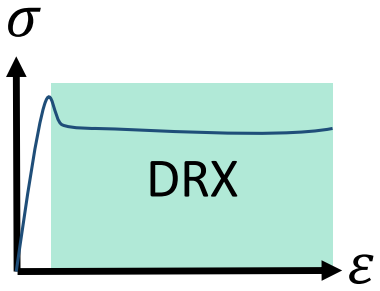

Boundary conditions from experimental data